International Journal of Mass Spectrometry 282 (2009) 123–127

Contents lists available at ScienceDirect

International Journal of Mass Spectrometry

journal homepage: www.elsevier.com/locate/ijms

Bismuth carbide cluster ions produced by a gas aggregation source

Y. Yamada*, T. Nakagawa

Department of Chemistry, Tokyo University of Science, 1-3 Kagurazaka, Shinjuku-ku, Tokyo 162-8601, Japan

ARTICLE INFO

Article history:
Received 19 September 2008
Received in revised form 16 February 2009
Accepted 16 February 2009
Available online 28 February 2009

Keywords:
Bismuth
Carbide
Cluster ion
Gas aggregation
Time-of-flight mass spectrometry

ABSTRACT

Bismuth carbide cluster ions, $Bi_nC_{2n}^+$ ($n = 3–11$), were produced using a gas aggregation source. Reactions of neutral Bi clusters with hydrocarbon gases having unsaturated C–C bonds (C_2H_2, C_2H_4, and $C_2H_2F_2$) followed by laser ionization can produce $Bi_nC_{2n}^+$ in a gas phase. Bismuth carbide clusters smaller than $Bi_3C_6^+$ were not found. Even-odd alternation in the stabilities of the cluster ions was observed, and the abundance of cluster ions with odd number of n in $Bi_nC_{2n}^+$ was enhanced in the TOF-mass spectra. Density functional calculations of the $Bi_nC_{2n}^+$ were performed in order to estimate the geometries of the cluster ions and the stability dependence on the cluster size.

1. Introduction

Metal carbides produced in a gas phase are attractive materials, particularly after the discovery of metalcarbohedrons (met-cars: metal–carbon species composed of metals bond to carbon) [1], because of their unique cage-like structures and chemical properties [2–4]. Metalcarbohedrons can be obtained for early transition metals (M_8C_{12}; M = Ti, Zr, Hf, V, Mb, Cr, and Mo). Investigations of other metal carbides, produced in a gas phase, without cage-like structures have also provided information on the bonding and chemical nature between carbon and metal atoms, which is important for applications such as catalysis and materials production [5–7]. The decomposition of hydrocarbons in the presence of a metal catalyst has been reported to produce carbon nanotubes [8,9]. Calculations on transition metal carbides clusters such as Ni_mC_n have been reported [10] in order to investigate the bonding nature of metals to graphite. The bonding natures of FeC_n [11–14], Co_xC_y [15,16], Mo_xC_y [17,18], Ti_xC_y [19], and Vi_xC_y [20] clusters have been reported on the basis of theoretical calculations. The production of metal carbide films is very important for applications. Pulsed laser ablation of Nd and Pr carbides was studied in order to obtain basic information on the deposition mechanism to form films [21], and laser ablation was found to mainly produce $(NdC_2)_n$ or $(PrC_2)_n$ clusters.

The formation of metal carbides in bulk is well known for early transition metals, whereas late-transition metals form carbides rather poorly. Therefore, it is useful to be able to produce late-transition metal carbides in the gas phase and to study their chemical properties. Carbide cluster anions C_nX^- of group-15 elements (X = N, P, As, Sb, and Bi) produced by laser ablation have been previously reported [22], and even-odd alternation of the cluster abundance was reported. Bi/C binary cluster ions, as well as other metal carbide cluster ions, have been produced using a laser ablation source [23]; the laser evaporation of a graphite rod coated with a film of bismuth metal produced Bi/C cluster ions, such as $Bi_2(C_3)_n^+$ ($n = 1–3$), $Bi_3C_3^+$, BiC_{10}^+, BiC_{12}^+, and BiC_{14}^+ clusters. While laser ablation is a popular method for producing compound cluster ions, gas aggregation is a suitable method for producing stable molecular clusters in the gas phase. We have previously reported that Bi/S clusters were produced by a gas aggregation source, and that unique structures such as Bi_6S_4 and Bi_6S_{11} were obtained reflecting the stability of the neutral molecule in the gas phase [24]. Copper carbide clusters, produced using a gas aggregation source, have also been reported previously [25], wherein C_2H_2 was passed over a heated crucible containing copper. In this study, bismuth carbide clusters were produced using a gas aggregation source and the clusters were characterized using TOF-mass spectrometry and density functional calculations.

2. Experimental

A gas aggregation source, which has been described previously [26], was employed for the cluster formation (Fig. 1). Bi powder in an alumina crucible was heated to approximately 600 K using a tungsten-heater and evaporated into a flow of He gas (0.5–1.5 standard L min^{-1}; slm). The gas mixture was cooled using a

---

* Corresponding author. Tel.: +81 3 5228 8276; fax: +81 3 3235 2214.
E-mail address: yyasu@rs.kagu.tus.ac.jp (Y. Yamada).

1387-3806/$ – see front matter © 2009 Elsevier B.V. All rights reserved.
doi:10.1016/j.ijms.2009.02.016

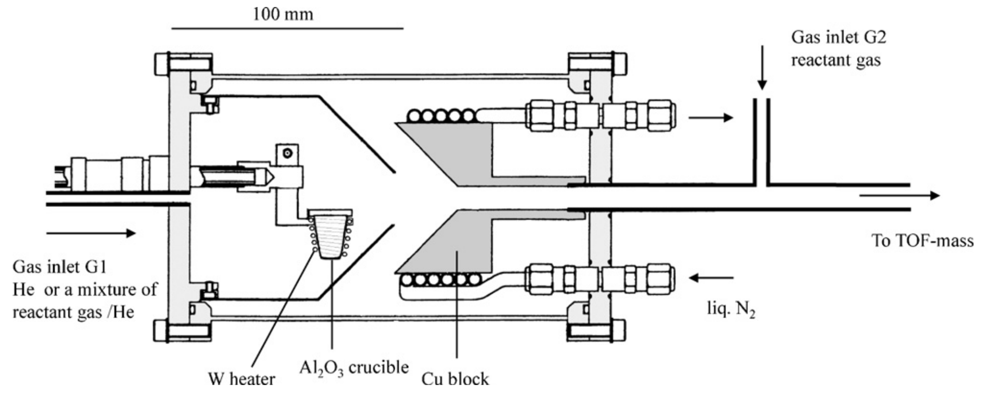

Fig. 1. Schematic of the gas aggregation cluster source.

cold Cu block (77 K), resulting in the formation of neutral clusters by aggregation. The gas sample was introduced into an ionization area through two skimmers in combination with a mechanical booster pump and two diffusion pumps. Neutral clusters were then ionized with fourth-harmonic light from a Nd:YAG laser (Minilite-II, HOYA Contimum, 266 nm, 10 Hz). The cluster ions were accelerated in an electric field (1.6 kV), passed through a 45-cm time-of-flight tube, and detected by a micro-channel plate (MCP) in an area evacuated by a turbo-molecular pump. The signals from the MCP were captured using a digital oscilloscope (LeCroy 9310A).

Hydrocarbon gases (C_2H_2, C_2H_4, C_2H_6, CH_4, C_6H_6, and CH_2CF_2) were introduced as reactant gases to produce the necessary carbide species. When a mixture of reactant gas and He carrier gas was introduced from the gas inlet G1, as shown in Fig. 1, the reactant gas thermally decomposed by contact with the W-heater to produce C atoms. On the other hand, when the reactant gas was introduced from the gas inlet G2 while He carrier gas was introduced from the gas inlet G1, the reactant gas did not contact the W-heater but only reacted with the neutral Bi clusters cooled to liquid N_2 temperature. Information on the production mechanism of the neutral clusters may be obtained by comparing the obtained cluster ions using these two gas introduction methods, though the subsequent laser ionization process caused fragmentation of neutral clusters.

3. Results and discussion

Pure Bi cluster ions were initially produced (before yielding bismuth carbide cluster ions) by not adding hydrocarbon gas to the He carrier gas. In the TOF-mass spectrum (Fig. 2), bismuth cluster ions Bi_n^+ were observed up to $n = 13$ having magic numbers at Bi_5^+ and Bi_7^+, reflecting their stability from the polyhedral skeletal electron pair theory (PSEPT) [24]; Bi_5^+ and Bi_7^+ correspond to *nido* and *arachno* in Wade's rule. Recently, density functional calculations for bismuth cluster cations have been reported [27], which are in agreement with our experimental results. Although the gas aggregation source produces neutral clusters, the TOF-mass spectra obtained after laser ionization reflect the stability of ionized clusters resulting from fragmentation of clusters caused by excess energy of ionizations.

In order to produce bismuth carbide clusters, hydrocarbon gases were added to the He carrier gas. The TOF-mass spectrum in Fig. 3 was obtained by vaporizing Bi while introducing a gas mixture of C_2H_2 and He from the same gas inlet G1. The hydrocarbon gases may be decomposed on the W-heater in the gas aggregation source to supply C atoms. While pure Bi cluster ions Bi_n^+ ($n = 1–5$) appeared in the spectrum, various bismuth carbide cluster ions were also produced. The compositions of the bismuth carbide cluster ions were $Bi_nC_{2n}^+$ ($n = 3–10$); no other compositions of Bi/C cluster ions were observed. If the Bi/C binary clusters were formed simply by aggregation of Bi and C atoms, then Bi/C binary cluster ions having compositions other than Bi/C = 1/2 ratio will be expected to be produced. The compositions observed may reflect the exclusive stable structures of the Bi/C cluster ions and provide clues regarding the formation mechanism of the cluster ions. Another remarkable

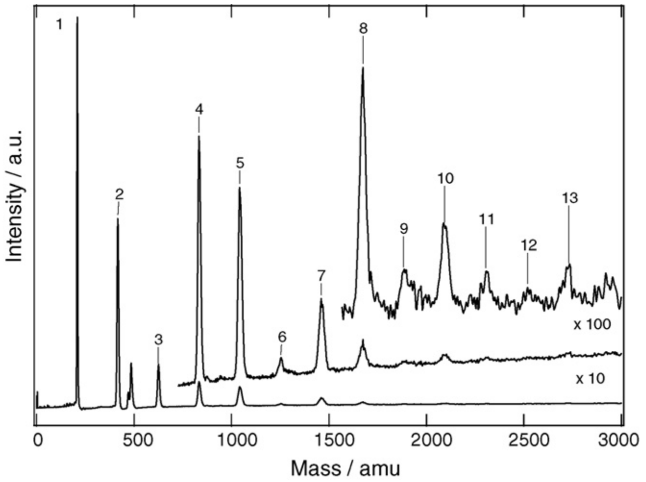

Fig. 2. Time-of-flight mass spectrum of Bi_n^+ cluster ions. The numbers correspond to n in Bi_n^+. The intensity of the signal in a large mass region is expanded (10 and 100 times). He gas (0.35 slm) was introduced as a carrier gas.

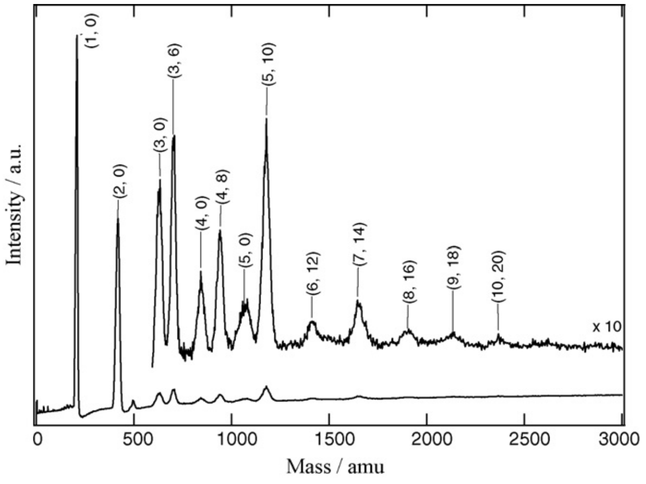

Fig. 3. Time-of-flight mass spectrum of $Bi_mC_n^+$ cluster ions obtained by the introduction of a mixture of He and C_2H_2 gas. The numbers correspond to $Bi_mC_n^+$; (m, n). Both He gas (0.26 slm) and C_2H_2 gas (0.15 slm) were introduced simultaneously from the gas inlet G1.

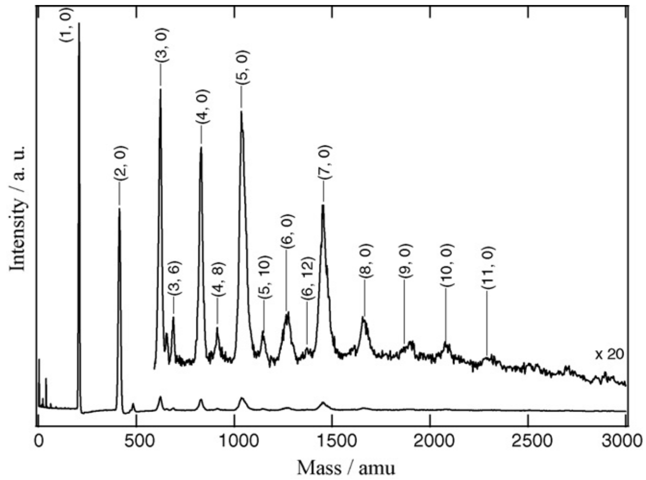

Fig. 4. Time-of-flight mass spectrum of $Bi_mC_n^+$ cluster ions obtained by the introduction of C_2H_2 gas after aggregation of neutral Bi_n in the He carrier gas. The numbers correspond to $Bi_mC_n^+$; (m, n). He gas (0.35 slm) and C_2H_2 gas (0.15 slm) were introduced from gas inlets G1 and G2, respectively.

point of interest is that the series of $Bi_nC_{2n}^+$ cluster ions starts at $Bi_3C_6^+$ ($n = 3$), and neither $Bi_1C_2^+$ nor $Bi_2C_4^+$ ($n = 1, 2$) was observed. If we assume that the Bi/C binary clusters are formed simply by attachment of C_2 units to the Bi cluster, $Bi_1C_2^+$ or $Bi_2C_4^+$ should be observed. The intensity of the $Bi_4C_8^+$ signal is weaker than that of the $Bi_3C_6^+$ and $Bi_5C_{10}^+$ signals. Similarly, the intensities of $Bi_nC_{2n}^+$ cluster ions with even number of Bi atoms (n) are weaker than those of neighboring $Bi_nC_{2n}^+$ cluster ions with odd number of Bi atoms.

In order to eliminate the effects of decomposition of C_2H_2 by the W-heater, C_2H_2 gas was introduced after the formation of neutral Bi_n clusters in the gas aggregation source. The He carrier gas was introduced from gas inlet G1 and the C_2H_2 reactant gas was introduced from gas inlet G2. The TOF-mass spectrum (Fig. 4) showed production of $Bi_nC_{2n}^+$ ($n = 3$–6), which was also obtained in previous experiments (Fig. 3), while the intensities of pure Bi_n^+ cluster ions are stronger than those of the $Bi_nC_{2n}^+$ cluster ions. It is presumed that the $Bi_x(C_2H_2)_y$ species may be the precursors of $Bi_nC_{2n}^+$ cluster ions; the neutral Bi_x clusters formed by aggregation reacted with C_2H_2 gas to form $Bi_x(C_2H_2)_y$ species in a gas phase. As the reaction $Bi_x + y(C_2H_2) \rightarrow Bi_x(C_2H_2)_y$ is enhanced by cooling, the yields of $Bi_nC_{2n}^+$ were enhanced when the C_2H_2 reactant gas was introduced from the gas inlet G1. Every Bi atom located on the surface of a Bi_n cluster can form a bond with a C_2H_2 molecule, and all of the Bi atoms in the Bi_n cluster in smaller sized regions ($n < 13$) are surface atoms. Neutral $Bi_x(C_2H_2)_y$ species were ionized by the laser irradiation, and the excess energy decomposed species to form $Bi_nC_{2n}^+$ cluster ions obtained in our experiments.

Next, C_2H_4 gas was added to the He carrier gas introduced through the gas inlet G1, and the spectra obtained using C_2H_4 were almost the same as those obtained using C_2H_2 (Fig. 3) when the amount of gas introduced was small (the flow rates of He and C_2H_2 gases were 0.26 slm and 0.05 slm, respectively). When the amount of C_2H_4/He introduced was increased (the flow rate of He and C_2H_2 gases was 0.41 slm and 0.12 slm, respectively), cluster ions having even number of Bi atoms disappeared while other series of Bi/C cluster ions, $Bi_5C_2^+$, $Bi_7C_6^+$, $Bi_9C_{10}^+$, and $Bi_{11}C_{14}^+$, were obtained, as seen in Fig. 5. Presumably, large sized neutral clusters, $Bi_x(C_2H_4)_y$, were produced due to increasing collision frequency between Bi atoms and C_2H_4 molecules. The enhanced fragmentation after laser ionization of $Bi_x(C_2H_4)_y$ could produce stable cluster ions $Bi_nC_{2n}^+$ in the small sized region ($n = 3$–9), as observed in the TOF-mass spectrum, and therefore the even-odd alternation of the abundance of $Bi_nC_{2n}^+$ was enhanced and new Bi/C cluster ions were produced. The new series of cluster ions starting from $Bi_5C_2^+$ can be expressed as $Bi_{5+2m}C_{2+4m}^+$ ($m = 0$–3), which have a smaller intensity than $Bi_nC_{2n}^+$ in the spectra.

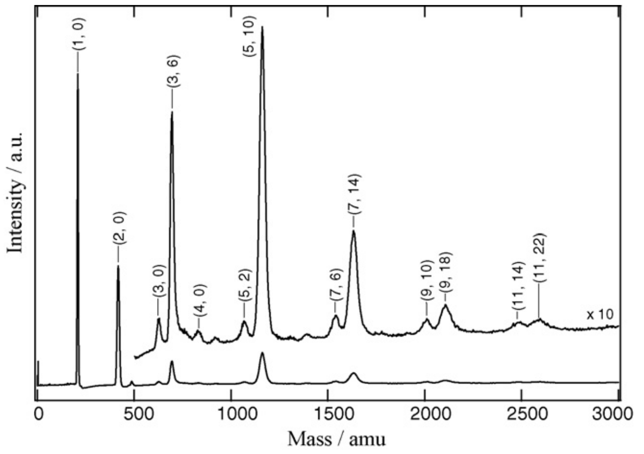

Fig. 5. Time-of-flight mass spectrum of $Bi_mC_n^+$ cluster ions obtained by the introduction of C_2H_4 gas. The numbers correspond to $Bi_mC_n^+$; (m, n). He gas (0.41 slm) and C_2H_4 gas (0.12 slm) were introduced simultaneously.

Considering that the precursor of $Bi_nC_{2n}^+$ cluster ions is either $Bi_x(C_2H_2)_y$ or $Bi_x(C_2H_4)_y$, the cluster ions produced by laser ionization and subsequent fragmentations might contain H atoms. In order to verify that the observed cluster ions do not contain H atoms, the TOF-mass spectra of $Bi_nC_{2n}^+$ produced by reactions with C_2H_2 and C_2H_4 under different experimental conditions were carefully compared. It was verified that the cluster ions did not contain H atoms, and the assignments were confirmed to be $Bi_nC_{2n}^+$. Furthermore, $C_2H_2F_2$ was employed as the reactant gas to form $Bi_nC_{2n}^+$ cluster ions, as the F atom has a sufficiently large mass to be distinguished in the TOF-mass spectra. In the TOF-mass spectrum (Fig. 6), Bi_n^+ and $Bi_nC_{2n}^+$ cluster ions were observed and no other signals assignable to species containing F atoms were found. It was thus proved that the cluster ions observed in this study are binary Bi/C cluster ions without H or F atoms.

Similar experiments were performed using CH_4, C_2H_6, and C_6H_6, and the obtained cluster ions were pure bismuth cluster ions, Bi_n^+; bismuth carbide Bi/C cluster ions were not observed. The unsaturated bond, C=C or C≡C, in a reactant hydrocarbon molecule is indispensable to yield Bi/C cluster ions. If the decomposition of the hydrocarbon to form C atoms by the W-heater is the precursor

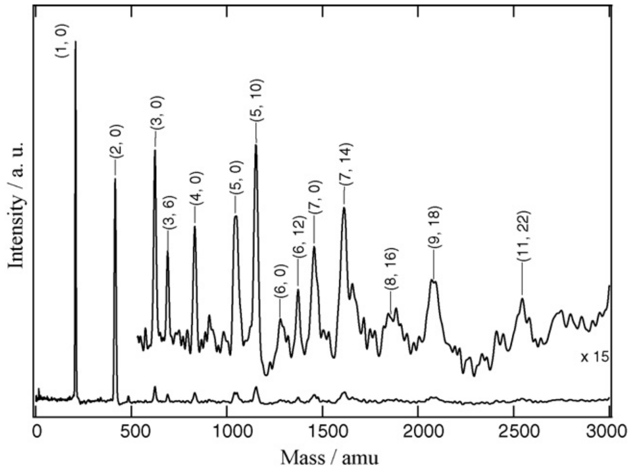

Fig. 6. Time-of-flight mass spectrum of $Bi_mC_n^+$ cluster ions obtained by the introduction of $C_2H_2F_2$ gas. The numbers correspond to $Bi_mC_n^+$; (m, n). He gas (0.34 slm) and $C_2H_2F_2$ gas (0.13 slm) were introduced simultaneously.

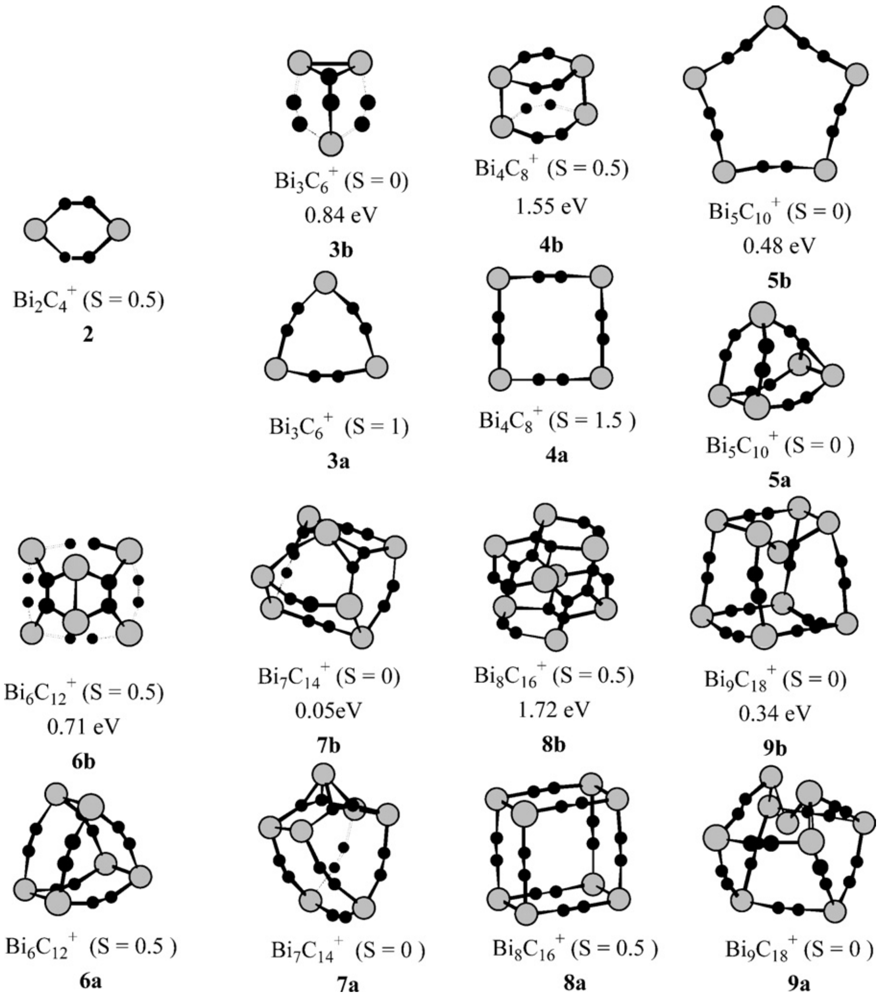

Fig. 7. The most stable structures of $Bi_nC_{2n}^+$ (n = 2–9) cluster ions calculated using ADF (ZORA/TZP) labeled with (a). For $Bi_nC_{2n}^+$ (n = 3–9) cluster ions, the isomers (b) are displayed along with relative bond energies to the corresponding most stable structures. The large gray balls and small black balls denote bismuth and carbon, respectively.

process for the production of bismuth carbide clusters, hydrocarbons without unsaturated bonds should also produce bismuth carbide clusters.

The major series of bismuth carbide cluster ions showing intense signals in the spectra had a composition of $Bi_nC_{2n}^+$, representing strong interaction between the Bi atom and the C_2 unit. Though decomposition of the neutral precursor $Bi_x(C_2H_2)_y$ species occurs after multi-photon laser ionization, the cluster ions produced ($Bi_nC_{2n}^+$) maintain the Bi/C ratio. If the bonding nature of the cluster ions is weak or the cluster structure consists of a Bi_x core, the composition of the cluster ions $Bi_xC_{2y}^+$ may have a distribution for the ratio of x and y. Though we performed the experiments under various conditions, BiC_2^+ and $Bi_2C_4^+$ were not obtained. These smaller cluster ions are too small to form stable structures. It can thus be concluded that the $Bi_nC_{2n}^+$ cluster ions have stable geometric structures resulting from the strong bonding between Bi atoms and C_2 units.

4. Density functional calculations

A density functional study of small neutral and cationic bismuth clusters has been previously reported [19], however calculations for bismuth carbide cluster ions have not yet been reported. We performed density functional calculations using the Amsterdam Density Functional (ADF) program package [28] to estimate the structure of the $Bi_nC_{2n}^+$ cluster ions obtained in the present study. Zero order regular approximation (ZORA) calculations were employed in order to include scalar relativistic effects with TZP (core double zeta, valence triple zeta, polarized basis sets) in the ADF program. The optimized structures are summarized in Fig. 7. From the experimental results, it may be assumed that the Bi/C cluster ions have C_2 units, and that the C_2 units are mixed with the same number of Bi atoms. First, calculations for the $Bi_3C_6^+$ cluster ion were performed assuming various initial structures, and it was found that the ring structure with S = 1 spin state is the most stable structure (Fig. 7-3a). The same ring structure with S = 0 spin state was found to be unstable; the binding energy was smaller by 0.77 eV than that of the structure with S = 1. The binding energy of $Bi_3C_6^+$ is larger than the sum of the energies of Bi_3^+ and C_6 (linear structure) by 1.45 eV, from a comparison of the calculated ground state energies. Generally, the Bi atom has three bonds in a molecule, and therefore, another isomer of the $Bi_3C_6^+$ cluster (Fig. 7-3b) in which each Bi atom connects with three atoms was calculated. This isomer has a Bi–Bi pair that may be stable in the low-spin S = 0 state; the Bi–Bi pair is considered to stabilize this cluster ion in the low-spin state. However, the ADF calculations show that the $Bi_3C_6^+$ isomer (Fig. 7-3b) was less stable by 0.84 eV compared to the most stable ring structure isomer with S = 1 (Fig. 7-3a). It was confirmed that the ring structure isomer $Bi_3C_6^+$, in which each Bi atom connects with only two C atoms, was the most stable structure, and that a Bi–Bi pair does not stabilize the cluster ion. Considering the formal charges and localized spins for the ring structure of $Bi_3C_6^+$ (S = 1), it is estimated that one Bi atom is responsible for the positive charge and the other two Bi atoms have two unpaired electrons, resulting

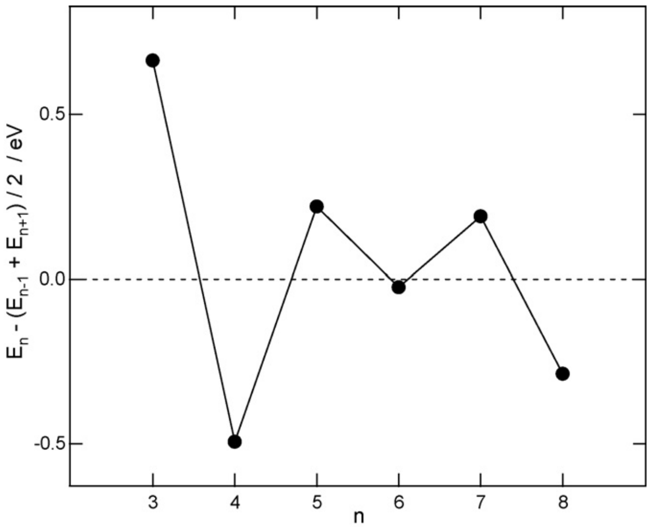

Fig. 8. Energy difference of $Bi_nC_{2n}^+$ cluster ions compared with the neighboring ions estimated using ADF (ZORA/TZP).

in the S = 1 spin state of the $Bi_3C_6^+$ cluster ion. However, the ADF calculations show that the three Bi atoms in the ring structure of $Bi_3C_6^+$ are equivalent.

$Bi_4C_8^+$ was also estimated to have a ring structure with S = 1.5 (Fig. 7-4a), in which four Bi atoms occupy the corner positions of a square. The structure with a higher spin state, S = 1.5, was estimated to be the most stable state, and the structure with a lower spin of S = 0.5 with the same structure was estimated to be unstable; it has 1.00 eV higher energy. The other structures with Bi–Bi bonds or Bi–C–Bi bonds, wherein each Bi atom has three bonds, were calculated to be unstable (Fig. 7-4b).

For $Bi_5C_{10}^+$, the ring structure was calculated assuming both S = 0 and 2, and the low-spin S = 0 (Fig. 7-5b) species were stable by 0.78 eV more than the high-spin S = 2 species. Both cluster ions, with S = 0 and 2, have almost the same optimized structures in which the Bi—C bond lengths are 2.17 Å and 2.20 Å, and the C═C bond lengths are 1.25 Å and 1.24 Å for the S = 0 and 2 species, respectively. It was demonstrated that the cluster ion without the Bi–Bi pair also stabilized in the low-spin state in the larger cluster ions, and that a Bi–Bi pair is not necessary as the origin of the stability of low-spin states. However, the structure shown in Fig. 7-5a was more stable by 0.48 eV than the ring structure with S = 0 (Fig. 7-5b). Calculations were also performed for the larger $Bi_nC_{2n}^+$ cluster ($n > 5$) assuming ring structures, however these ring structures were found to be unstable. The most stable structure of the $Bi_6C_{12}^+$ cluster (Fig. 7-6a) consists of two Bi_3C_6 rings, which has the S = 0.5 spin state. The $Bi_7C_{14}^+$ (S = 0; Fig. 7-7a) cluster ion has a similar structure as $Bi_6C_{12}^+$ in which one Bi atom is located between two C═C bonds and one C═C unit is inserted into one Bi–Bi bond. $Bi_8C_{16}^+$ (S = 0.5; Fig. 7-8a) has a structure consisting of two Bi_4C_8 rings. $Bi_9C_{18}^+$ (S = 0; Fig. 7-9a) has a structure similar to $Bi_8C_{16}^+$ wherein one Bi atom bonds to two Bi atoms in the ring. It was found that the lowest spin states, S = 0 (when n = odd) or S = 0.5 (when n = even), are preferable for the large $Bi_nC_{2n}^+$ clusters ($n > 4$).

In the $Bi_nC_{2n}^+$ ($n > 2$) series, even-odd alternation of the abundance in the TOF-mass spectra was observed, and the cluster ions with odd number of n in $Bi_nC_{2n}^+$ were more stable than neighboring clusters with even number of $n + 1$ and $n - 1$. In order to quantify the stability of the cluster ions, the calculated bonding energies E_n for $Bi_nC_{2n}^+$ were compared. Though $Bi_2C_4^+$ was not observed in our experiment, calculations for the $Bi_2C_4^+$ cluster ion (Fig. 7-2) were performed in order to make a comparison with a neighboring $Bi_3C_6^+$ cluster ion. The bonding energy E_n of the ground state structures for $Bi_nC_{2n}^+$ was estimated by geometry optimization using the ADF program. The stability of $Bi_nC_{2n}^+$ compared with neighboring cluster ions ($Bi_{n+1}C_{2(n+1)}^+$ and $Bi_{n-1}C_{2(n-1)}^+$) by the energy difference $E_n - (E_{n-1} + E_{n+1})/2$ shows the even-odd alternation (Fig. 8); cluster ions having an odd number of Bi atoms were more stable than the neighboring cluster ions having an even number of Bi atoms. This is in agreement with the intensities of the species in the observed TOF-spectra.

5. Conclusions

Bismuth carbide cluster ions, $Bi_nC_{2n}^+$, were produced using a gas aggregation source. When C_2H_2 was employed as a reactant gas, the precursors of the cluster ions were neutral $Bi_x(C_2H_2)_y$. Subsequent multi-photon laser ionization followed by fragmentation produced $Bi_nC_{2n}^+$. The composition of the bismuth carbide is exclusively $Bi_nC_{2n}^+$ and no other composition was found. $Bi_3C_6^+$ is the smallest cluster ion in the $Bi_nC_{2n}^+$ series. $Bi_nC_{2n}^+$ having odd number of Bi atoms was found to be stable. Density functional calculations indicated that $Bi_3C_6^+$ and $Bi_4C_8^+$ have ring structures with a high-spin state, while the larger cluster ions $Bi_nC_{2n}^+$ ($n > 5$) had low-spin states without ring structures. The even-odd alternation in the stability of $Bi_nC_{2n}^+$ was also demonstrated by the density functional calculations.

References

[1] B.C. Guo, K.P. Kerns, A.W. Castleman Jr., Science 255 (1992) 1411.
[2] S.-G. He, Y. Xie, F. Dong, E.R. Bernstein, J. Chem. Phys. 125 (2006) 164306.
[3] J.M. Lightstone, M.J. Patterson, P. Liu, M.G. White, J. Phys. Chem. A 110 (2006) 3505.
[4] P. Liu, J.M. Lightstone, M.J. Patterson, J.A. Rodriguez, J.T. Muckerman, M.G. White, J. Phys. Chem. B 110 (2006) 7449.
[5] D.S. Bethune, C.H. Kiang, M.S. de Vries, G. Gorman, R. Savoy, J. Vazquez, R. Beyers, Nature 363 (1993) 605.
[6] M.A. Duncan, J. Cluster Sci. 8 (1997) 239.
[7] S. Iijima, T. Ichihashi, Nature 363 (1993) 603.
[8] J.H. Hafner, M.J. Bronikowski, B.R. Azamian, P. Nikolaev, A.G. Rinzler, D.T. Colbert, K.A. Smith, R.E. Smalley, Chem. Phys. Lett. 296 (1998) 195.
[9] Y. Shibuta, S. Maruyama, Comput. Mater. Sci. 39 (2007) 842.
[10] A.N. Andriotis, M. Menon, G.E. Froudakis, J.E. Lowther, Chem. Phys. Lett. 301 (1999) 503.
[11] M.F.A. Hendrickx, S. Clima, Chem. Phys. Lett. 388 (2004) 290.
[12] M.V. Ryzhkov, A.L. Ivanovskii, B.T. Delley, Chem. Phys. Lett. 404 (2005) 400.
[13] E.G. Noya, R.C. Longo, L.J. Gallego, J. Chem. Phys. 119 (2003) 11131.
[14] A.V. Arbuznikov, M. Hendrickx, L.G. Vanquickenborne, Chem. Phys. Lett. 310 (1999) 515.
[15] P. Redondo, C. Barrientos, A. Largo, Int. J. Mass Spectrom. 272 (2008) 187.
[16] K. Tono, A. Terasaki, T. Ohta, T. Kondow, J. Chem. Phys. 117 (2002) 7010.
[17] H. Tominaga, M. Nagai, Appl. Catal. A: General 282 (2005) 5.
[18] J.M. Lightstone, H.A. Mann, M. Wu, P.M. Johnson, M.G. White, J. Phys. Chem. B 107 (2003) 10359.
[19] Y. Yuan, K. Deng, Y. Liu, C. Tang, W. Tan, D. Huang, J. Yang, X. Wang, J. Chem. Phys. 128 (2008) 064314.
[20] K.L. Knappenberger Jr., C.E. Jones Jr., M.A. Sobhy, I. Iordanov, J. Sofo, A.W. Castleman Jr., J. Phys. Chem. A 110 (2006) 12814.
[21] R. Teghil, L. D'Alessio, A. Satagata, D. Ferro, G. De Maria, Appl. Surf. Sci. 208 (2003) 119.
[22] R.B. Huang, C.R. Wang, Z.Y. Liu, L.S. Zheng, F. Qi, L.S. Sheng, S.Q. Yu, Y.W. Zhang, Z. Phys. D 33 (1995) 49.
[23] J.E. Reddic, M.A. Duncan, Chem. Phys. Lett. 264 (1997) 157.
[24] Y. Yamada, Chem. Lett. 2001 (2001) 1126.
[25] Y. Yamada, A.W. Castleman Jr., Chem. Phys. Lett. 204 (1993) 133.
[26] T. Fujiwara, A. Iizuka, K. Sato, Y. Yamada, Int. J. Mass Spectrom. 242 (2005) 57.
[27] H.K. Yuan, H. Chen, A.L. Kuang, Y. Miao, Z.H. Xiong, J. Chem. Phys. 128 (2008) 94305.
[28] E.J. Baerends, J. Autschbach, A. Bérces, F.M. Bickelhaupt, C. Bo, P.M. Boerrigter, L. Cavallo, D.P. Chong, L. Deng, R.M. Dickson, D.E. Ellis, M. van Faassen, L. Fan, T.H. Fischer, C. Fonseca Guerra, S.J.A. van Gisbergen, J.A. Groeneveld, O.V. Gritsenko, M. Grüning, F.E. Harris, P. van den Hoek, C.R. Jacob, H. Jacobsen, L. Jensen, G. van Kessel, F. Kootstra, E. van Lenthe, D.A. McCormack, A. Michalak, J. Neugebauer, V.P. Nicu, V.P. Osinga, S. Patchkovskii, P.H.T. Philipsen, D. Post, C.C. Pye, W. Ravenek, P. Ros, P.R.T. Schipper, G. Schreckenbach, J.G. Snijders, M. Solà, M. Swart, D. Swerhone, G. te Velde, P. Vernooijs, L. Versluis, L. Visscher, O. Visser, F. Wang, T.A. Wesolowski, E.M. van Wezenbeek, G. Wiesenekker, S.K. Wolff, T.K. Woo, A.L. Yakovlev, T. Ziegler, Amsterdam Density Functional software package, ADF2007.01, SCM, Theoretical Chemistry, Vrije Universiteit, Amsterdam, The Netherlands, http://www.scm.com.